Optimal joint remote state preparation in the presence of various types of noises

You may also be interested in:

Optimal joint remote state preparation in the presence of various types of noises

Van Hop Nguyen[1]**, Thi Bich Cao**[2] **and Ba An Nguyen**[2]

[1] Department of Physics, Hanoi National University of Education, 136 Xuan Thuy, Cau Giay, Hanoi, Vietnam
[2] Center for Theoretical Physics, Institute of Physics, Vietnam Academy of Science and Technology, 18 Hoang Quoc Viet, Cau Giay, Hanoi, Vietnam

E-mail: nban@iop.vast.vn

CrossMark

Abstract

A main obstacle faced by any quantum information processing protocol is the noise that degrades the desired coherence/entanglement. In this work we study by means of Kraus operators the effect of four typical types of noises on the quality of joint remote state preparation of a single-qubit state using a three-qubit Greenberger–Horne–Zeilinger-type state as the initial quantum channel. Assuming that two of the three involved qubits independently suffer a type of noise, we derive analytical expressions not only for the optimal averaged fidelities but also for the boundaries in phase space of the domains in which the joint remote state preparation protocol outperforms the classical one. Detailed discussion is given for each of the total 16 noisy scenarios. We also provide physical interpretation for the obtained results and outline possible future topics.

1. Introduction

Joint remote state preparation (JRSP) is a global protocol [1–3] in which a group of M people, called the preparers, remotely cooperate to provide a quantum state $|\psi\rangle$ for another distant person, called the receiver, in such a way so as to meet two following prerequisite conditions: (i) only local operations and classical communication are allowed and (ii) any individual one or any subgroup of the preparers cannot infer the full information encoded in the state $|\psi\rangle$. The condition (i) is ensured by sharing among the preparers and the receiver a proper multipartite entangled resource. As for the condition (ii), the full classical information of $|\psi\rangle$ is secretly divided into M pieces, each of which is independently given

to a preparer. Such a secret information splitting makes JRSP secure compared to remote state preparation (RSP) protocols (see e.g. [4]) in which there is only one preparer who catches the entire information about $|\psi\rangle$. Technically, JRSP and RSP just require single-qubit von Neumann measurements so they are less demanding than quantum teleportation [5] that needs collective Bell-measurements. Since its introduction a great deal of papers on JRSP has been published in diverse aspects [6–23]. In its early development, only probabilistic protocols were devised [1–3, 6–10, 13–16, 18, 21–24]. Later it turns out that JRSP can be made deterministic by adopting adaptive measurement strategies [11, 17, 19, 20] (i.e. the preparers carry out their measurements in sequence with the outcome of an earlier measuring preparer being feed forwarded to a next preparer who will make use of it to choose the right basis for his/her own measurement). JRSP is also approached to from an experimental architecture point of view [25] and, recently, a scheme for realizing JRSP of photonic states with linear-optics devices has been proposed [26].

Adv. Nat. Sci.: Nanosci. Nanotechnol. **8** (2017) 015012

V H Nguyen *et al*

Like other quantum tasks, JRSP suffers a serious problem under the name decoherence caused by unavoidable interactions with surrounding noisy environments during the preliminary stage of entanglement distribution that make an intended quantum channel pure state become mixed one with lesser degree of entanglement. If the source of quantum resources is generous, special procedures can be applied to distill a desired state from an ensemble of decohered states, provided that fidelity of the decohered states with respect to the desired state is not too low (namely, not smaller than 1/2) [27–31]. However, distillation procedures consume a heavy overheads in both quantum resource/technology and time. A possible way out of the situation is to directly employ the decohered state. In this perspective, studying the effect of noises is truly necessary to optimize the performance of a given quantum protocol. A few authors already devoted their interest to noisy JRSP using different kinds of shared quantum channels through Lindblad master equations within the framework of Markov-Born approximations [32–35]. In this work, motivated by the study in [36] for noisy quantum teleportation, we shall resort to the apparatus of Kraus operators to investigate similar issues but with respect to JRSP. A particular new result compared with previous works is that besides analytical expressions for the optimal averaged fidelities we also derive expressions in terms of noise strengths for the boundaries of the domains in which quality of the JRSP protocol is better than that achievable by any classical means. Note that very recently the authors of [37] have used the same mathematical apparatus to deal with the same topic but with simpler noisy scenarios, so their results are contained in ours as particular cases.

We structure our paper in four sections. In the next section, section 2, we shall for clarity present the general formalism of the $M = 2$ JRSP of a single-qubit state in density matrix language. Section 3 will analyze in detail various scenarios of four standard noise types acting on two of the three qubits of concern. Each scenario has its own consequences which will be elucidated in due places in section 3. The final conclusion section, section 4, will summarize our results with physical interpretations and briefly list on what could be done subsequently.

2. General formalism

Consider a case when there are two preparers (Alice and Bob) and what to be remotely prepared is a single-qubit state of the most general form

$$|\psi\rangle = \cos\frac{\vartheta}{2}|0\rangle + \sin\frac{\vartheta}{2}e^{i\varphi}|1\rangle, \qquad (1)$$

with $\vartheta \in [0, \pi]$ and $\varphi \in [0, 2\pi]$. Alice knows only ϑ, while Bob knows only φ, so neither of them knows $|\psi\rangle$. The quantum channel shared beforehand among the two preparers and the receiver (Charlie) is in general an entangled mixed state ρ_{123}, with qubit 1 (2, 3) held by Alice (Bob, Charlie). The joint remote preparation of $|\psi\rangle$ begins with Alice who measures qubit 1 in the basis $\{|u_k\rangle_1; \ k = 0, 1\}$,

$$\begin{pmatrix} |u_0\rangle_1 \\ |u_1\rangle_1 \end{pmatrix} = U(\vartheta) \begin{pmatrix} |0\rangle_1 \\ |1\rangle_1 \end{pmatrix}, \qquad (2)$$

with $U(\vartheta)$ a specific unitary operator depending on ϑ and on the initial condition. If her measurement outcome is k (i.e. $|u_k\rangle_1$ is found), qubit 1 is disentangled from ρ_{123} but Bob's and Charlie's qubits remain entangled with their state being in the form

$$\rho_{23}^{(k)} = \frac{{}_1\langle u_k|\rho_{123}|u_k\rangle_1}{P^{(k)}}, \qquad (3)$$

where

$$P^{(k)} = Tr_{23}({}_1\langle u_k|\rho_{123}|u_k\rangle_1) \qquad (4)$$

is the probability of Alice's obtaining the outcome k. Next, conditioned on Alice's announced measurement outcome, Bob measures qubit 2 in the basis $\left\{\left|v_l^{(k)}\right\rangle_2; \ l = 0, 1\right\}$,

$$\begin{pmatrix} \left|v_0^{(k)}\right\rangle_2 \\ \left|v_1^{(k)}\right\rangle_2 \end{pmatrix} = V^{(k)}(\varphi) \begin{pmatrix} |0\rangle_2 \\ |1\rangle_2 \end{pmatrix}, \qquad (5)$$

where $V^{(k)}(\varphi)$ is a specific unitary operator depending not only on φ but also on k. If Bob finds $\left|v_l^{(k)}\right\rangle_2$ (i.e. his outcome is l which should also be publicly announced), state $\rho_{23}^{(k)}$ becomes separable: $\rho_{23}^{(k)} \to \left|v_l^{(k)}\right\rangle_2 \left\langle v_l^{(k)}\right| \otimes \rho_3^{(kl)}$, with

$$\rho_3^{(kl)} = \frac{{}_2\left\langle v_l^k\left|\rho_{23}^{(k)}\right|v_l^k\right\rangle_2}{P^{(kl)}}, \qquad (6)$$

where

$$P^{(kl)} = Tr_3\left({}_2\left\langle v_l^{(k)}\left|\rho_{23}^{(k)}\right|v_l^{(k)}\right\rangle_2\right) \qquad (7)$$

is the probability of Bob's obtaining the outcome l. Finally, after collecting the measurement outcomes k and l announced by Alice and Bob, Charlie applies on $\rho_{23}^{(k)}$ a suitable unitary operator $R^{(kl)}$ to obtain the state

$$\widetilde{\rho}^{(kl)} = R^{(kl)}\rho_3^{(kl)}(R^{(kl)})^+, \qquad (8)$$

whose fidelity in comparison with the desired state $|\psi\rangle$ in equation (1) is determined by

$$F^{(kl)} = \langle\psi|\widetilde{\rho}^{(kl)}|\psi\rangle. \qquad (9)$$

Averaging over the four possible measurement outcomes yields

$$F = \sum_{k=0}^{1}\sum_{l=0}^{1} P^{(k)}P^{(kl)}F^{(kl)}. \qquad (10)$$

Generally, F depends on the quantum channel and the state to-be-prepared, so to have a state-independent fidelity we further average over all the possible parameters of the input state. Assuming a uniform distribution, the state-independent averaged fidelity $\langle F\rangle$ can be calculated following the formula

$$\langle F\rangle = \frac{1}{4\pi}\int_0^\pi d\vartheta \, \sin\vartheta \int_0^{2\pi} d\varphi F, \qquad (11)$$

whose dependence on the quantum channel however remains.

3. Effects of noises

It is ideal if there are no noises and the initial quantum channel is a pure maximally entangled state which is not unique but may be Einstein–Podolski–Rosen (EPR) states [2, 3, 6, 11–13, 17, 20], Greenberger–Horne–Zeilinger (GHZ) state [1–3, 6–8, 15, 19], W state [9, 10, 14] or others [16, 18, 21–24]. In case it is the GHZ state $|Q\rangle_{123} = (|0\,0\,0\rangle + |1\,1\,1\rangle)_{123}/\sqrt{2}$ [38], the unitary operators in equations (2) and (5) are chosen as

$$U(\vartheta) = \begin{pmatrix} \cos\dfrac{\vartheta}{2} & \sin\dfrac{\vartheta}{2} \\ \sin\dfrac{\vartheta}{2} & -\cos\dfrac{\vartheta}{2} \end{pmatrix} \qquad (12)$$

and

$$V^{(k)}(\varphi) = \frac{1}{\sqrt{2}}\begin{pmatrix} (-1)^k e^{-ik\varphi} & e^{-i(1-k)\varphi} \\ e^{-ik\varphi} & (-1)^{1-k} e^{-i(1-k)\varphi} \end{pmatrix}. \quad (13)$$

Then, $R^{(kl)} = X^k Z^l$, with $X = \{\{0,1\},\{1,0\}\}$ and $Z = \{\{1,0\}, \{0,-1\}\}$ being the well-known Pauli matrices. This results in $F^{(kl)} = 1$ for any k, l, ϑ and φ, implying perfect JRSP. Here, in the presence of noises, we employ the initial quantum channel in the form

$$|Q(\theta)\rangle_{123} = \left(\cos\theta|0\,0\,0\rangle + \sin\theta|1\,1\,1\rangle\right)_{123}, \qquad (14)$$

with θ introduced as a freely controlling parameter to optimize the JRSP performance.

The effect of noises can conveniently be accounted for by means of superoperators whose action on a density matrix yields again a legitimate density matrix. In the operator-sum representation the mentioned superoperator is given in terms of Kraus operators [39] which adequately model a specific type of noise. Four typical noise types which are often encountered in reality are bit-flip (B), phase-flip (P), amplitude-damping (A) and depolarizing (D) (the physical meaning of a noise type can be found in [39, 40]). Suppose that each of the qubits 1, 2, 3 independently experiences a type of noise. Subjected to such noise types, the initial pure quantum channel state $|Q(\theta)\rangle_{123}$ in equation (14) becomes a mixed one, ρ_{123}, which can be represented in terms of Kraus operators as

$$\rho_{123}^{\alpha\beta\gamma} = \sum_{j=1}^{N_\alpha}\sum_{m=1}^{N_\beta}\sum_{n=1}^{N_\gamma} K_j^\alpha(p_{1\alpha}) \otimes K_m^\beta(p_{2\beta}) \otimes K_n^\gamma(p_{3\gamma})|Q(\theta)\rangle_{123}\langle Q(\theta)|$$
$$K_j^{\alpha+}(p_{1\alpha}) \otimes K_m^{\beta+}(p_{2\beta}) \otimes K_n^{\gamma+}(p_{3\gamma}), \qquad (15)$$

where $K_j^\alpha(p_{1\alpha})$ and $p_{1\alpha}$ are the jth Kraus operator and the noise strength for qubit 1 under the action of the noise type $\alpha \in \{B, P, A, D\}$, while N_α is the number of α-type noise Kraus operators. The noise strength is a parameterized quantity which is proportional to the time the noise is acting on the qubit or the distance the qubit has to travel along in the noisy environment. If the time/distance is zero the noise strength is zero. Infinity of the time/distance is meant by unit noise strength. Hence, $p_{1\alpha}$ satisfies the conditions $0 \leqslant p_{1\alpha} \leqslant 1$

and is in essence a probability. Similar explanations hold for $K_m^\beta(p_{2\beta}), K_n^\gamma(p_{3\gamma})$, $p_{2\beta}$, $p_{3\gamma}$ and N_β, N_γ. Let Bob be capable of producing the initial quantum channel $|Q(\theta)\rangle_{123}$ at his well-equipped laboratory. After that, he keeps qubit 2 with himself in a noise-free storage, but sends qubit 1 (3) to Alice (Charlie) via α-type (γ-type) noisy environment. Hence, the resulting channel reduces to

$$\rho_{123}^{\alpha\gamma} = \sum_{j=1}^{N_\alpha}\sum_{n=1}^{N_\gamma} K_j^\alpha(p_{1\alpha}) \otimes I \otimes K_n^\gamma(p_{3\gamma})|Q(\theta)\rangle_{123}\langle Q(\theta)|$$
$$K_j^{\alpha+}(p_{1\alpha}) \otimes I \otimes K_n^{\gamma+}(p_{3\gamma}), \qquad (16)$$

with $I = \{\{1, 0\}, \{0, 1\}\}$ being the identity operator.

First, consider $\alpha = B$ and $\gamma \in \{B, P, A, D\}$. The Kraus operators of interest are well-known:

$$K_1^B(p_{nB}) = \sqrt{1 - p_{nB}}\, I, \quad K_2^B(p_{nB}) = \sqrt{p_{nB}}\, X, \qquad (17)$$

$$K_1^P(p_{nP}) = \sqrt{1 - p_{nP}}\, I, \quad K_2^P(p_{nP}) = \sqrt{p_{nP}}\, Z, \qquad (18)$$

$$K_1^A(p_{nA}) = \begin{pmatrix} 1 & 0 \\ 0 & \sqrt{1 - p_{nA}} \end{pmatrix}, \quad K_2^A(p_{nA}) = \begin{pmatrix} 0 & \sqrt{p_{nA}} \\ 0 & 0 \end{pmatrix} \qquad (19)$$

and

$$K_1^D(p_{nD}) = \sqrt{1 - \frac{3}{4}p_{nD}}\, I, \quad K_2^D(p_{nD}) = \sqrt{\frac{1}{4}p_{nD}}\, X,$$
$$K_3^D(p_{nD}) = i\sqrt{\frac{1}{4}p_{nD}}\, XZ, \quad K_4^D(p_{nD}) = \sqrt{\frac{1}{4}p_{nD}}\, Z. \qquad (20)$$

Calculations based on the above formulae for the Kraus operators and those given in the general formalism section give

$$\langle F_{BB}\rangle = \frac{2}{3} - \frac{1}{3}\left[p_{1B} + p_{3B} - 2p_{1B}p_{3B} - (1 - p_{3B})\sin(2\theta)\right], \qquad (21)$$

$$\langle F_{BP}\rangle = \frac{2}{3} - \frac{1}{3}\left[p_{1B} - (1 - 2p_{3P})\sin(2\theta)\right], \qquad (22)$$

$$\langle F_{BA}\rangle = \frac{2}{3} - \frac{1}{3}\left[p_{1B} + (1 - 2p_{1B})p_{3A}\sin^2\theta - \sqrt{1 - p_{3A}}\,\sin(2\theta)\right] \qquad (23)$$

and

$$\langle F_{BD}\rangle = \frac{2}{3} - \frac{1}{6}\left[2p_{1B} + p_{3D} - 2p_{1B}p_{3D} - 2(1 - p_{3D})\sin(2\theta)\right]. \qquad (24)$$

At this moment the parameter θ introduced in equation (14) will play its role. Since $0 \leqslant p_{n\alpha} \leqslant 1$ for any $n \in \{1, 2, 3\}$ and $\alpha \in \{B, P, A, D\}$, it is trivial from equations (21), (22) and (24) that the optimal values of θ at which $\langle F_{BB}\rangle, \langle F_{BP}\rangle$ and $\langle F_{BD}\rangle$ become maximal are

$$\theta_{\mathrm{opt}}^{BB} = \theta_{\mathrm{opt}}^{BD} = \frac{\pi}{4}, \qquad (25)$$

$$\theta_{\mathrm{opt}}^{BP} = \begin{cases} \pi/4 & \text{for } p_{3P} < 1/2, \\ -\pi/4 & \text{for } p_{3P} > 1/2. \end{cases} \qquad (26)$$
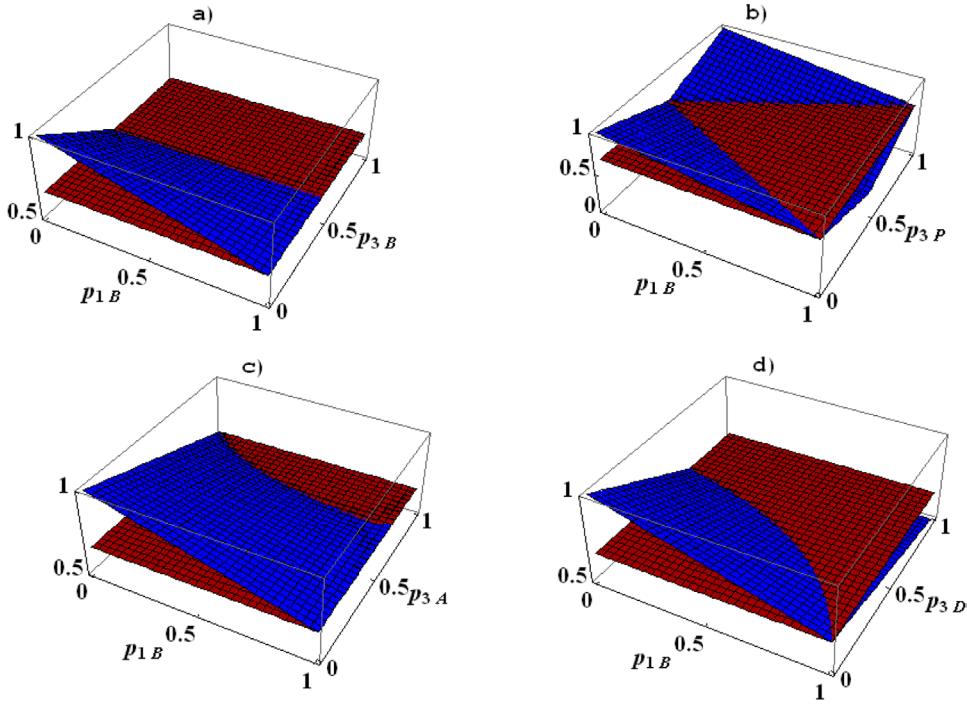
Figure 1. The optimal averaged fidelity (a) $\langle F_{BB}\rangle_{\mathrm{opt}}$, (b) $\langle F_{BP}\rangle_{\mathrm{opt}}$, (c) $\langle F_{BA}\rangle_{\mathrm{opt}}$ and (d) $\langle F_{BD}\rangle_{\mathrm{opt}}$ as a function of p_{1B} and $p_{3\gamma}$ ($\gamma = B, P, A, D$). The plane at 2/3 is inserted to help visualizing the quantum ($\langle F_{B\gamma}\rangle_{\mathrm{opt}} > 2/3$) and classical ($\langle F_{B\gamma}\rangle_{\mathrm{opt}} \leqslant 2/3$) domains.

Yet, nontrivial is the case of $\langle F_{BA}\rangle$ in equation (23). The optimal value $\theta_{\mathrm{opt}}^{BA}$ that makes $\langle F_{BA}\rangle$ maximal can be determined from the equation $\partial\langle F_{BA}\rangle/\partial\theta\big|_{\theta=\theta_{\mathrm{opt}}^{BA}}= 0$ and the condition $\partial^2\langle F_{BA}\rangle/\partial\theta^2\big|_{\theta=\theta_{\mathrm{opt}}^{BA}} < 0$. Solving this equation with the condition we have

$$\theta_{\mathrm{opt}}^{BA} = \frac{1}{2}\arctan\frac{2\sqrt{1-p_{3A}}}{(1-2p_{1B})p_{3A}}. \qquad (27)$$

With so chosen values of $\theta_{\mathrm{opt}}^{B\gamma}$ we have straightforwardly derived the optimal averaged fidelities $\langle F_{B\gamma}\rangle_{\mathrm{opt}}$ from equations (21)–(24). Their analytical expressions read

$$\langle F_{BB}\rangle_{\mathrm{opt}} = 1 - \frac{1}{3}(p_{1B} + 2p_{3B} - 2p_{1B}p_{3B}), \qquad (28)$$

$$\langle F_{BP}\rangle_{\mathrm{opt}} = \frac{2}{3} - \frac{1}{3}(p_{1B} - |1 - 2p_{3P}|), \qquad (29)$$

$\langle F_{BA}\rangle_{\mathrm{opt}}$
$$= \frac{2}{3} - \frac{1}{6}\left[2p_{1B} + 3p_{3A} - 2p_{1B}p_{3A} - \sqrt{4(1-p_{3A}) + (1-2p_{1B})^2 p_{3A}^2}\right]$$
$$\qquad (30)$$
and

$$\langle F_{BD}\rangle_{\mathrm{opt}} = 1 - \frac{1}{6}(2p_{1B} + 3p_{3D} - 2p_{1B}p_{3D}). \qquad (31)$$

The dependences of $\langle F_{B\gamma}\rangle_{\mathrm{opt}}$ on p_{1B} and $p_{3\gamma}(\gamma = B, P, A, D)$ are plotted in figure 1. As a rule, the JRSP protocol is useless if the optimal averaged fidelities $\langle F_{B\gamma}\rangle_{\mathrm{opt}}$ is equal to or smaller than 2/3, the best classically achievable fidelity value [41, 42].

To visualize the domain of p_{1B} and $p_{3\gamma}$ within which the JRSP protocol remains useful we display in figure 2 the corresponding density plots in phase spaces. As quickly followed from figures 1(a) and 2(a), $\langle F_{BB}\rangle_{\mathrm{opt}}$ decreases with increasing p_{1B} or/and p_{3B}. A closer look, however, reveals that if $p_{1B} = 1$ then $\langle F_{BB}\rangle_{\mathrm{opt}} = 2/3$ for any p_{3B}, whereas for any given $p_{1B} < 1$, the quality of JRSP is getting worse though still acceptable ($\langle F_{BB}\rangle_{\mathrm{opt}} > 2/3$) as p_{3B} is increasing from zero. However, the protocol suddenly loses its usefulness at $p_{3B} = 1/2$ at which $\langle F_{BB}\rangle_{\mathrm{opt}} = 2/3$ and beyond which $\langle F_{BB}\rangle_{\mathrm{opt}} < 2/3$. That is, p_{3B} should be smaller than 1/2 to keep the JRSP protocol superior to the classical one. Yet, for any $p_{3B} < 1/2$ the value of $\langle F_{BB}\rangle_{\mathrm{opt}}$ is tending to 2/3 only asymptotically with increasing p_{1B}. Differently from $\langle F_{BB}\rangle_{\mathrm{opt}}$, the behavior of $\langle F_{BP}\rangle_{\mathrm{opt}}$ seems unusual. Notice that $\langle F_{BP}\rangle_{\mathrm{opt}}$ is always equal to or less than 2/3 when $p_{3P} = 1/2$ for any p_{1B}, i.e. the necessary condition for the JRSP to be useful is $p_{3P} \neq 1/2$. Moreover, for a given $p_{3P} < 1/2(p_{3P} > 1/2)$, $\langle F_{BP}\rangle_{\mathrm{opt}}$ is first decreases with increasing p_{1B} until $p_{1B} = 1 - 2p_{3P}$ ($2p_{3P} - 1$), at which $\langle F_{BP}\rangle_{\mathrm{opt}}$ drops to 2/3, and then the protocol ceases to work for any further increase in p_{1B}. On the other hand, for a given p_{1B} the value of $\langle F_{BP}\rangle_{\mathrm{opt}}$ decreases as p_{3P} increases from zero, which is usual. This tendency continues until $p_{3P} = (1 - p_{1B})/2$, at and immediately beyond which the protocol 'dies' (i.e. out of service). Interestingly, however, as p_{3P} increases further to reach a value larger than $(1 + p_{1B})/2$ the protocol 'revives' (i.e. back to service) with $\langle F_{BP}\rangle_{\mathrm{opt}}$ increasing with p_{3P}, which seems unusual since it would mean that '*more noise better quality*' (i.e. larger p_{3P} leads to larger $\langle F_{BP}\rangle_{\mathrm{opt}}$). Such sudden 'death' and sudden 'birth' of service of the quantum JRSP protocol for $\langle F_{BP}\rangle_{\mathrm{opt}}$ are
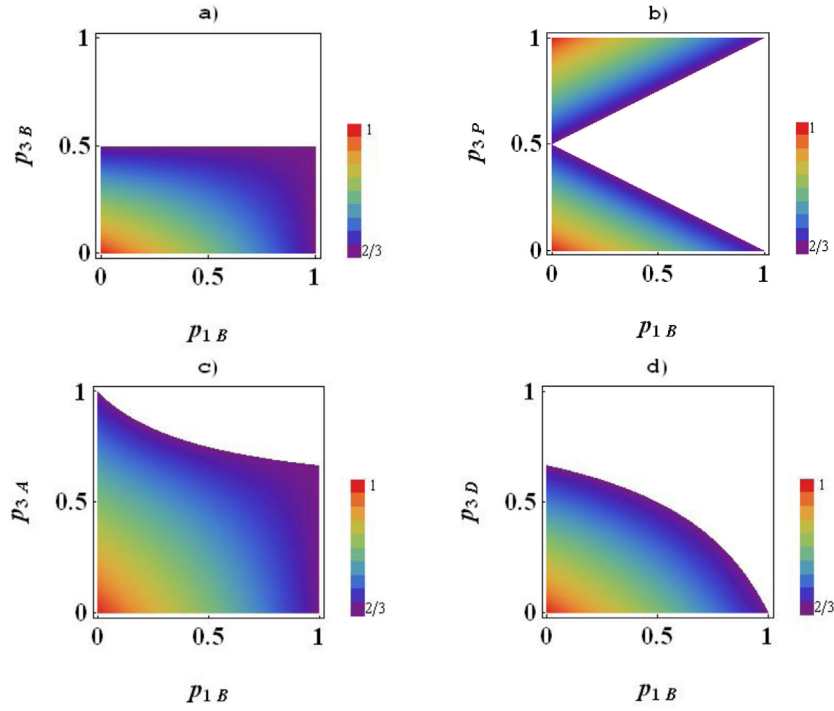
Figure 2. Phase diagrams for the optimal averaged fidelity (a) $\langle F_{BB} \rangle_{\mathrm{opt}}$, (b) $\langle F_{BP} \rangle_{\mathrm{opt}}$, (c) $\langle F_{BA} \rangle_{\mathrm{opt}}$ and (d) $\langle F_{BD} \rangle_{\mathrm{opt}}$ in the $p_{1B} - p_{3\gamma}$ space. The magnitude of $\langle F_{B\gamma} \rangle_{\mathrm{opt}}$ is described by colors. The classical domain is in white backgrounds.

clearly seen from figures 1(b) and 2(b). Figures 1(c) and 2(c) show that adding more noise, either bit-flip noise or noise due to amplitude-damping mechanism or both, always reduces the JRSP efficiency. Qualitatively, this is somewhat similar to the case in figures 1(a) and 2(a), except the fact that the upper bound $p_{3A}^{\max}$ of the strength of noise acting on qubit 3 is not a constant but a function of p_{1B}, i.e. $p_{3A}^{\max} = (1 + p_{1B})/(1 + 2p_{1B})$, which monotonically decreases with p_{1B}. In particular, a seeming surprise arises here if we look back at the expression of $\theta_{\mathrm{opt}}^{BA}$ in equation (27) which indicates that $\theta_{\mathrm{opt}}^{BA} \neq \pi/4 (\theta_{\mathrm{opt}}^{BA} = \pi/4)$ when $p_{3A} \neq 0 (p_{3A} = 0)$. This says that non-maximally entangled channel ($|Q(\theta \neq \pi/4)\rangle_{123}$) outperforms maximally entangled channel ($|Q(\theta = \pi/4)\rangle_{123}$) or '*less entanglement better quality*'. As for figures 1(d) and 2(d), the useful domain in phase space is narrower than that in figures 1(c) and 2(c), with the border determined by $p_{3D} = 2(1 - p_{1B})/(3 - 2p_{1B})$ or $p_{1B} = (3p_{3D} - 2)/[2(p_{3D} - 1)]$.

Next, consider $\alpha = P$ and $\gamma \in \{B, P, A, D\}$. In this scenario the values of θ that make the JRSP protocol optimal can be found to be

$$\theta_{\mathrm{opt}}^{PB} = \theta_{\mathrm{opt}}^{PD} = \begin{cases} \pi/4 & \text{for } p_{1P} < 1/2, \\ -\pi/4 & \text{for } p_{1P} > 1/2, \end{cases} \quad (32)$$

$$\theta_{\mathrm{opt}}^{PP} = \begin{cases} \pi/4 & \text{for } p_{1P} < 1/2, \ p_{3P} < 1/2 \text{ or } p_{1P} > 1/2, \ p_{3P} > 1/2, \\ -\pi/4 & \text{for } p_{1P} < 1/2, \ p_{3P} > 1/2 \text{ or } p_{1P} > 1/2, \ p_{3P} < 1/2, \end{cases} \quad (33)$$

$$\theta_{\mathrm{opt}}^{PA} = \frac{1}{2} \arctan \frac{2(1 - 2p_{1P})\sqrt{1 - p_{3A}}}{p_{3A}}. \quad (34)$$

Note that use of the above value of $\theta_{\mathrm{opt}}^{PA}$ reduces the entanglement degree of the initial quantum channel $|Q(\theta)\rangle_{123}$ in equation (14). The optimal averaged fidelities are derived in the form

$$\langle F_{PB} \rangle_{\mathrm{opt}} = \frac{2}{3} + \frac{|1 - 2p_{1P}|(1 - p_{3B}) - p_{3B}}{3}, \quad (35)$$

$$\langle F_{PP} \rangle_{\mathrm{opt}} = \frac{2}{3} + \frac{|(1 - 2p_{1P})(1 - 2p_{3P})|}{3}, \quad (36)$$

$$\langle F_{PA} \rangle_{\mathrm{opt}} = \frac{2}{3} + \frac{\sqrt{4(1 - 2p_{1P})^2(1 - p_{3A}) + p_{3A}^2} - p_{3A}}{6} \quad (37)$$

and

$$\langle F_{PD} \rangle_{\mathrm{opt}} = \frac{2}{3} + \frac{2|1 - 2p_{1P}|(1 - p_{3D}) - p_{3D}}{6}. \quad (38)$$

The dependences of $\langle F_{P\gamma} \rangle_{\mathrm{opt}}$ on p_{1P} and $p_{3\gamma}$ ($\gamma = B, P, A, D$) are plotted in figure 3 and the phase-space useful domains are shown in figure 4. The border between the useful and useless domains for $\langle F_{PB} \rangle_{\mathrm{opt}}$ in figure 4(a) obeys the equation $p_{3B} = |1 - 2p_{1P}|/(1 + |1 - 2p_{1P}|)$. So $p_{3B} \geqslant 1/2$ are ruled out. For a $p_{3B} < 1/2$, $\langle F_{PB} \rangle_{\mathrm{opt}}$ first decreases with p_{1P} until $p_{1P}^{\min} = 1/[2(1 + p_{3B})]$ at which it gets equal to 2/3. The segment of p_{1P} sandwiched between $p_{1P}^{\min}$ and $p_{1P}^{\max} = (1 + 2p_{3B})/[2(1 + p_{3B})]$ is irrelevant, but after $p_{1P}^{\max}$ the JRSP protocol becomes more and more efficient with increasing phase-flip noise. When qubit 1 is affected by phase-flip noise and qubit 3 (a) also by phase-flip noise or (b) by amplitude-damping noise, the protocol is better than the
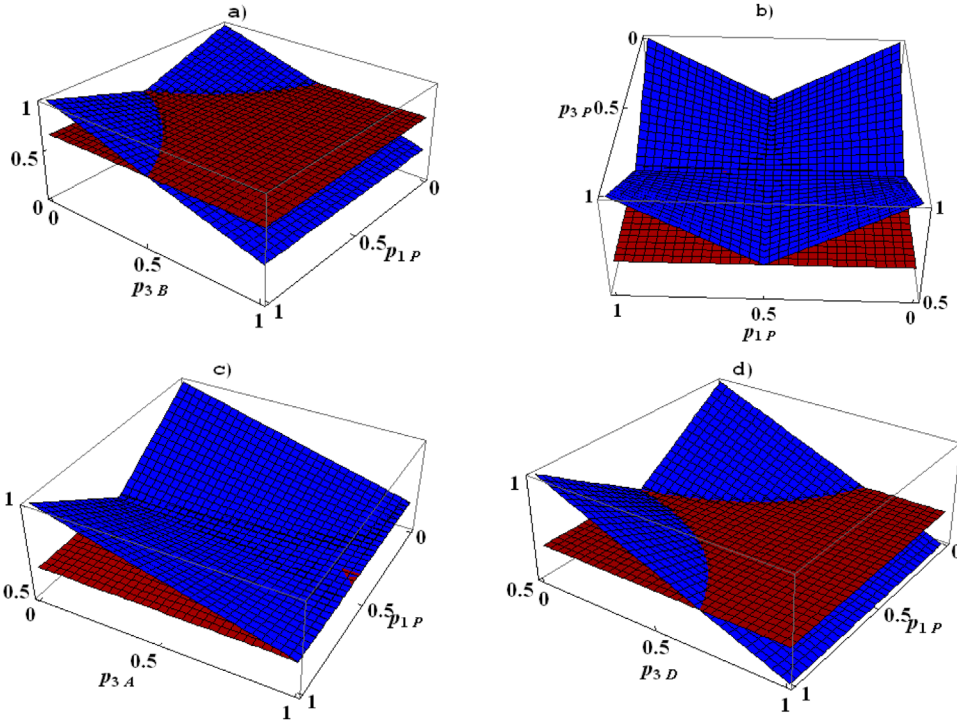
Figure 3. The optimal averaged fidelity (a) $\langle F_{PB} \rangle_{\mathrm{opt}}$, (b) $\langle F_{PP} \rangle_{\mathrm{opt}}$, (c) $\langle F_{PA} \rangle_{\mathrm{opt}}$ and (d) $\langle F_{PD} \rangle_{\mathrm{opt}}$ as a function of p_{1P} and $p_{3\gamma}$ ($\gamma = B, P, A, D$). The plane at 2/3 is inserted to help visualizing the quantum ($\langle F_{P\gamma} \rangle_{\mathrm{opt}} > 2/3$) and classical ($\langle F_{P\gamma} \rangle_{\mathrm{opt}} \leqslant 2/3$) domains.
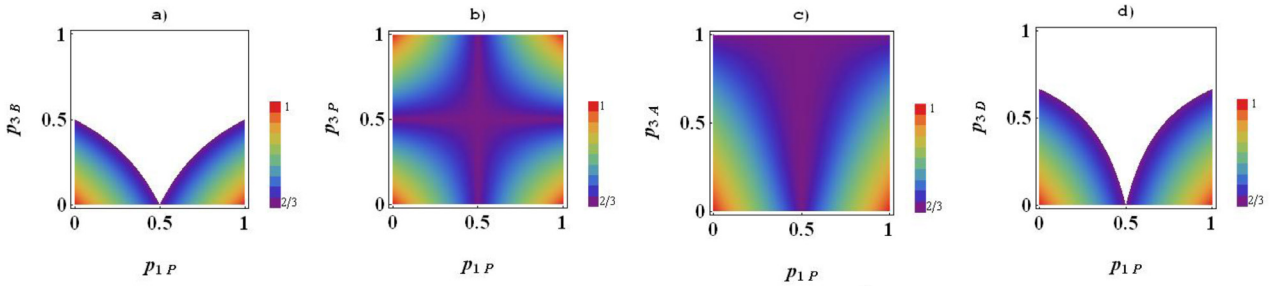

Figure 4. Phase diagrams for the optimal averaged fidelity (a) $\langle F_{PB} \rangle_{\mathrm{opt}}$, (b) $\langle F_{PP} \rangle_{\mathrm{opt}}$, (c) $\langle F_{PA} \rangle_{\mathrm{opt}}$ and (d) $\langle F_{PD} \rangle_{\mathrm{opt}}$ in the $p_{1P} - p_{3\gamma}$ space. The magnitude of $\langle F_{P\gamma} \rangle_{\mathrm{opt}}$ is described by colors. The classical domain is in white backgrounds.

classical one for almost all the values of noise strengths. In fact, for the case (a) it requires only $p_{1P} \neq 1/2$ and $p_{3P} \neq 1/2$, while for the case (b) only $p_{1P} \neq 1/2$ and $p_{3A} \neq 1$, as is evident from figures 4(b) and (c). When qubit 1 is affected by phase-flip noise and qubit 3 by depolarizing noise, the phase-space diagram shown in figure 4(d) is similar to that in figure 4(a), but with the border described by a different equation, $p_{3D} = 2|1 - 2p_{1P}|/(1 + 2|1 - 2p_{1P}|)$, so that of p_{3D} cannot be equal to or greater than 2/3 and for a given $p_{3D} < 2/3$ the values of p_{1P} should be smaller than $(2 + p_{3B})/[4(1 + p_{3B})]$ or greater than $(2 + 3p_{3B})/[4(1 + p_{3B})]$.

Further, consider $\alpha = A$ and $\gamma \in \{B, P, A, D\}$. The optimal values of θ are found to be

$$\theta_{\mathrm{opt}}^{AB} = \frac{1}{2} \arctan \frac{2\sqrt{1 - p_{1A}}(1 - p_{3B})}{p_{1A}(1 - 2p_{3B})}, \qquad (39)$$

$$\theta_{\mathrm{opt}}^{AP} = \frac{1}{2} \arctan \frac{2\sqrt{1 - p_{1A}}(1 - 2p_{3P})}{p_{1A}}, \qquad (40)$$

$$\theta_{\mathrm{opt}}^{AA} = \frac{1}{2} \arctan \frac{2\sqrt{(1 - p_{1A})(1 - p_{3A})}}{p_{1A} + p_{3A} - 2p_{1A}p_{3A}} \qquad (41)$$

and

$$\theta_{\mathrm{opt}}^{AD} = \frac{1}{2} \arctan \frac{2\sqrt{1 - p_{1A}}}{p_{1A}}. \qquad (42)$$

With any of the above $\theta_{\mathrm{opt}}^{A\gamma}$ the initial quantum channel $|Q(\theta)\rangle_{123}$ is non-maximally entangled but the corresponding averaged fidelities are maximal

$$\langle F_{AB} \rangle_{\mathrm{opt}} = \frac{1}{6} \Big[4 - p_{1A} - 2p_{3B} + 2p_{1A}p_{3B}$$
$$+ \sqrt{4(1 - p_{1A})(1 - p_{3B})^2 + p_{1A}^2 (1 - 2p_{3B})^2} \Big], \qquad (43)$$

$$\langle F_{AP} \rangle_{\mathrm{opt}} = \frac{1}{6} \Big[4 - p_{1A} + \sqrt{p_{1A}^2 + 4(1 - p_{1A})(1 - 2p_{3P})^2} \Big], \qquad (44)$$
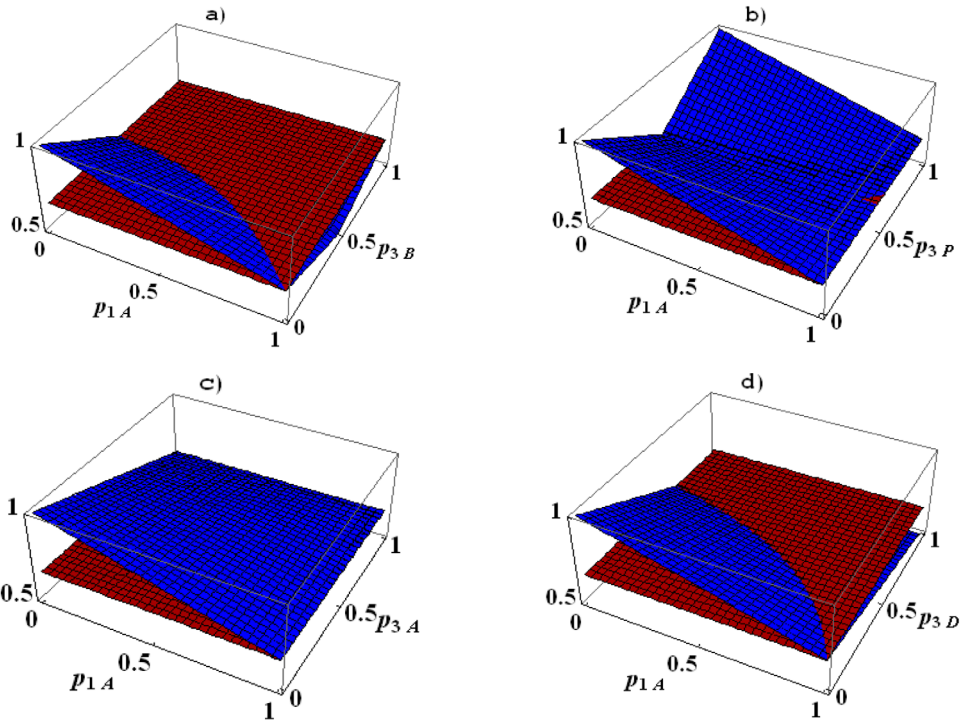
Adv. Nat. Sci.: Nanosci. Nanotechnol. **8** (2017) 015012

V H Nguyen *et al*

Figure 5. The optimal averaged fidelity (a) $\langle F_{AB}\rangle_{\rm opt}$, (b) $\langle F_{AP}\rangle_{\rm opt}$, (c) $\langle F_{AA}\rangle_{\rm opt}$ and (d) $\langle F_{AD}\rangle_{\rm opt}$ as a function of p_{1A} and $p_{3\gamma}$ ($\gamma = B, P, A, D$). The plane at 2/3 is inserted to help visualizing the quantum ($\langle F_{A\gamma}\rangle_{\rm opt} > 2/3$) and classical ($\langle F_{A\gamma}\rangle_{\rm opt} \leqslant 2/3$) domains.
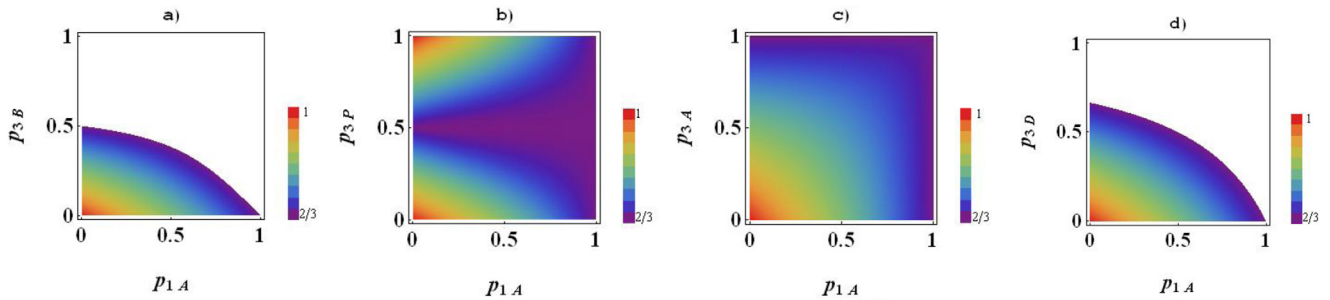

Figure 6. Phase diagrams for the optimal averaged fidelity (a) $\langle F_{AB}\rangle_{\rm opt}$, (b) $\langle F_{AP}\rangle_{\rm opt}$, (c) $\langle F_{AA}\rangle_{\rm opt}$ and (d) $\langle F_{AD}\rangle_{\rm opt}$ in the $p_{1A} - p_{3\gamma}$ space. The magnitude of $\langle F_{A\gamma}\rangle_{\rm opt}$ is described by colors. The classical domain is in white backgrounds.

$$\langle F_{AA}\rangle_{\rm opt} = \frac{1}{6}\Big[4 - p_{1A} - p_{3A} + 2p_{1A}p_{3A}$$
$$+ \sqrt{4(1 - p_{1A})(1 - p_{3A}) + (p_{1A} + p_{3A} - 2p_{1A}p_{3A})^2}\,\Big]$$

and $\hspace{10cm}$ (45)

$$\langle F_{AD}\rangle_{\rm opt} = \langle F_{BD}\rangle_{\rm opt}. \tag{46}$$

Note that although the precise calculations yield different expressions for the averaged fidelities (i.e. $\langle F_{AD}\rangle \neq \langle F_{BD}\rangle$) and the corresponding optimal values of θ also differ (i.e. $\theta_{\rm opt}^{AD} \neq \theta_{\rm opt}^{BD}$) the optimization procedure brings about equal optimal averaged fidelities (i.e. $\langle F_{AD}\rangle_{\rm opt} = \langle F_{BD}\rangle_{\rm opt}$). Figures 5 and 6 show the dependences of $\langle F_{A\gamma}\rangle_{\rm opt}$ on p_{1A} and $p_{3\gamma}$ ($\gamma = B, P, A, D$) and the corresponding phase-space diagrams. The quantum–classical border in figure 6(a) is described by the

equation $p_{3B} = \Big(2 - p_{1A} - \sqrt{4 - 8p_{1A} + 5p_{1A}^2}\,\Big)/(2p_{1A})$, while that in figure 6(d) is of the form as in figure 2(d). Qualitatively the diagrams in figures 6(a) and (d) are similar, but quantitatively they differ in areas and the values at $p_{1A} = 0$. When qubit 3 is subjected to phase-flip (amplitude-damping) noise all of p_{1A} and p_{3P} are relevant, except for $p_{3P} = 1/2$ ($p_{3A} = 1$), as visual in figure 6(b) (figure 6(c)).

Finally, consider $\alpha = D$ and $\gamma \in \{B, P, A, D\}$. Straightforward calculations yield

$$\theta_{\rm opt}^{DB} = \theta_{\rm opt}^{DD} = \frac{\pi}{4}, \tag{47}$$

and

$$\theta_{\rm opt}^{DP} = \begin{cases} \pi/4 \text{ for } p_{3P} < 1/2 \\ -\pi/4 \text{ for } p_{3P} > 1/2 \end{cases} \tag{48}$$

Adv. Nat. Sci.: Nanosci. Nanotechnol. **8** (2017) 015012

V H Nguyen *et al*

Figure 7. The optimal averaged fidelity (a) $\langle F_{DB} \rangle_{\mathrm{opt}}$, (b) $\langle F_{DP} \rangle_{\mathrm{opt}}$, (c) $\langle F_{DA} \rangle_{\mathrm{opt}}$ and (d) $\langle F_{DD} \rangle_{\mathrm{opt}}$ as a function of p_{1D} and $p_{3\gamma}$ ($\gamma = B, P, A, D$). The plane at 2/3 is inserted to help visualizing the quantum ($\langle F_{D\gamma} \rangle_{\mathrm{opt}} > 2/3$) and classical ($\langle F_{D\gamma} \rangle_{\mathrm{opt}} \leqslant 2/3$) domains.
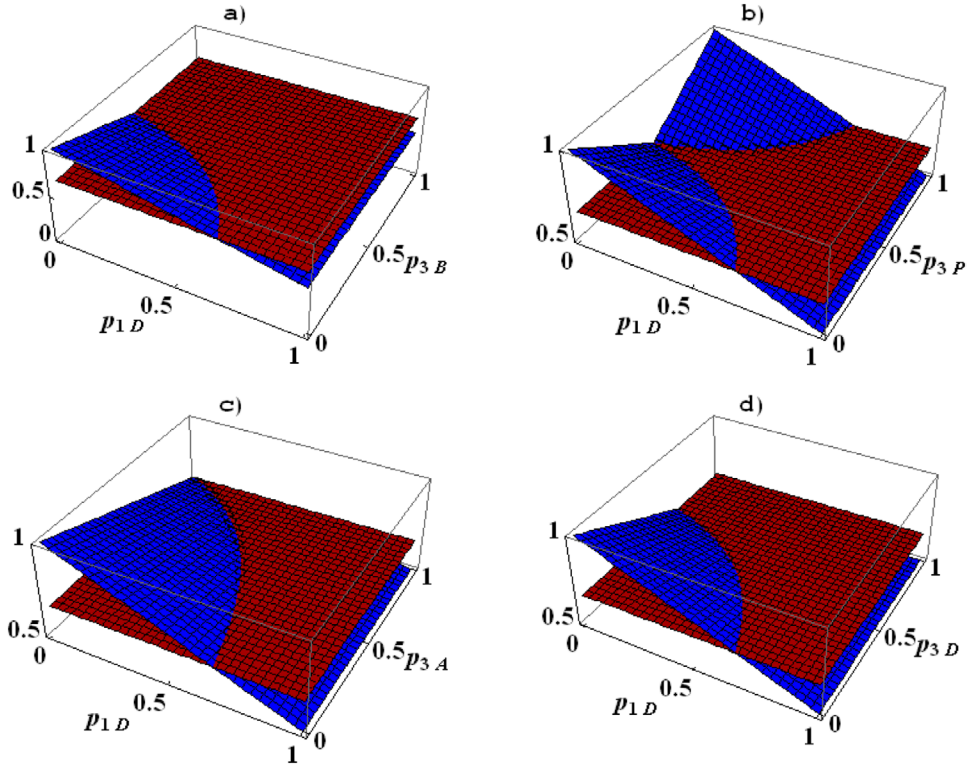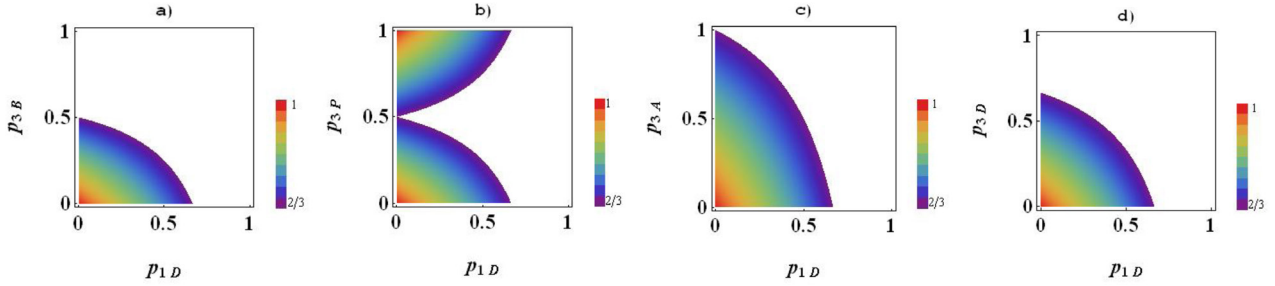

Figure 8. Phase diagrams for the optimal averaged fidelity (a) $\langle F_{DB} \rangle_{\mathrm{opt}}$, (b) $\langle F_{DP} \rangle_{\mathrm{opt}}$, (c) $\langle F_{DA} \rangle_{\mathrm{opt}}$ and (d) $\langle F_{DD} \rangle_{\mathrm{opt}}$ in the $p_{1D} - p_{3\gamma}$ space. The magnitude of $\langle F_{D\gamma} \rangle_{\mathrm{opt}}$ is described by colors. The classical domain is in white backgrounds.

$$\theta_{\mathrm{opt}}^{DA} = \frac{1}{2} \arctan \frac{2\sqrt{1 - p_{3A}}}{p_{3A}}. \tag{49}$$

The optimal averaged fidelities are derived in the form

$$\langle F_{DB} \rangle_{\mathrm{opt}} = 1 - \frac{2p_{3B}}{3} - \frac{p_{1D}(3 - 4p_{3B})}{6}, \tag{50}$$

$$\langle F_{DP} \rangle_{\mathrm{opt}} = \frac{2}{3} - \frac{p_{1D}}{6} + \frac{(1 - p_{1D})|1 - 2p_{3P}|}{3}, \tag{51}$$

$$\langle F_{DA} \rangle_{\mathrm{opt}} = 1 - \frac{p_{3A}}{3} - \frac{p_{1D}(3 - 2p_{3A})}{6} \tag{52}$$

and

$$\langle F_{DD} \rangle_{\mathrm{opt}} = 1 - \frac{p_{3D}}{2} - \frac{p_{1D}(1 - p_{3D})}{2}. \tag{53}$$

The optimal averaged fidelity $\langle F_{DB} \rangle_{\mathrm{opt}}$ ($\langle F_{DP} \rangle_{\mathrm{opt}}$, $\langle F_{DA} \rangle_{\mathrm{opt}}$ and $\langle F_{DD} \rangle_{\mathrm{opt}}$) as a function of p_{1D} and P_{3B} (P_{3P}, P_{3A} and P_{3D}) is displayed in figure 7.

The equations of the quantum–classical border in figures 8(a) and (b) are given by $p_{3B} = (2 - 3p_{1D})/[4(1 - p_{1D})]$ and $p_{3P} = (2 - p_{1D})/[4(1 - p_{1D})]$, while those in figures 8(c) and (d) are of the form $p_{3A} = (2 - 3p_{1D})/[2(1 - p_{1D})]$ and $p_{3D} = (2 - 3p_{1D})/[3(1 - p_{1D})]$. The phase-space diagrams in figure 8 tell that generally the allowed values of p_{1D} and $p_{3\gamma}$ are more limited in this scenario compared with those previously considered.

4. Conclusion

We have drawn a small stroke in the big picture of decoherence by analyzing how noises affect the quality of JRSP using a controllable GHZ-type state as the initial quantum

channel. The types of noises we have considered are bit-flip, phase-flip, amplitude-damping and depolarizing noise which are usually met in realistic situations. The action of a noise type on a qubit is modeled by a superoperator in terms of the operator-sum of Kraus operators. We assumed that two of the three concerned qubits are acted on by an independent noise and derived explicit dependences of optimal averaged fidelities of JRSP in all possible 16 scenarios. In each scenario we also figured out the phase space diagrams allowing to specify the range of noise strengths in which the quantum JRSP protocol is better than the best classical one. Beside the usually expected property that quality gets worse with increasing noise or/ and decreasing degree of entanglement, we encountered two 'unusual' things. The first one is '*more noise better quality*' and the second one is '*less entanglement better quality*'. These things also arose in noisy quantum teleportation [36] as a direct result of mathematical calculations. Here we provide physical interpretations. The point is that quality is decided by the working quantum channel state. In the presence of noises the working state is the decohered one but not the initial one. More concretely, in the context of our JRSP protocol, the working state is $\rho_{123}^{\alpha\gamma}(\theta)$ in equation (16) but not the initial one $\left|Q(\theta)\right\rangle_{123}$ in equation (14). Because the ideal state $\left|Q(\theta = \pi/4)\right\rangle_{123}$ is maximally entangled, it is natural that the closer $\rho_{123}^{\alpha\gamma}(\theta)$ is to $\left|Q(\theta = \pi/4)\right\rangle_{123}\left\langle Q(\theta = \pi/4)\right|$ the better quality of JRSP results. As can be verified, under the action of phase-flip noise the closeness between $\rho_{123}^{\alpha\gamma}(\theta)$ and $\left|Q(\theta = \pi/4)\right\rangle_{123}\left\langle Q(\theta = \pi/4)\right|$ is maximal if $\theta = -\pi/4$ when the noise strength is larger than 1/2. By choosing such θ for the initial state $\left|Q(\theta)\right\rangle_{123}$ the entanglement degree contained in the working state $\rho_{123}^{\alpha\gamma}(\theta)$ increases with the noise strength when it is larger than 1/2. Hence, the '*more noise better quality*' is physically translated to '*larger entanglement better quality*' (note, here it is entanglement of the working channel $\rho_{123}^{\alpha\gamma}(\theta = -\pi/4)$. Likewise, under the action of amplitude-damping noise the closeness between $\rho_{123}^{\alpha\gamma}(\theta)$ and $\left|Q(\theta = \pi/4)\right\rangle_{123}\left\langle Q(\theta = \pi/4)\right|$ is maximal at $\theta \neq \pi/4$. That is, the initial state $\left|Q(\theta \neq \pi/4)\right\rangle_{123}$ is non-maximally entangled, but the entanglement degree of the working state $\rho_{123}^{\alpha\gamma}(\theta \neq \pi/4)$ is larger than the entanglement degree of $\rho_{123}^{\alpha\gamma}(\theta = \pi/4)$. So, the '*less entanglement better quality*' also implies '*larger entanglement better quality*' (note, in the former italic sentence entanglement means entanglement of the initial quantum channel but in the latter italic sentence entanglement means entanglement of the decohered quantum channel which is the working one). Therefore, in light of our interpretations the two 'unusual' things mentioned above turn out to be usual: both in fact reflect the truth that a working (not initial) quantum channel with a larger degree of entanglement results in a better quality of JRSP protocol. For a comprehensive study one can extend this work to the case when all the three qubits are subjected to noises or to consider other kinds of the initial quantum channels or analyze other ways of noise action (e.g. collective action of different types of noises, non-Markovian noise, etc). Noisy JRSP and noisy controlled JRSP of multi-qubit states are also worth investigating. These topics may be dealt with in future.

References

[1] Xia Y, Song J and Song H S 2007 *J. Phys. B: At. Mol. Opt. Phys.* **40** 3719
[2] An N B and Kim J 2008 *J. Phys. B: At. Mol. Opt. Phys.* **41** 095501
[3] An N B and Kim J 2008 *Int. J. Quantum Inf.* **6** 1051
[4] Pati A K 2000 *Phys. Rev.* A **63** 014302
    Nguyen B A, Cao T B, Nung V D and Kim J 2011 *Adv. Nat. Sci.: Nanosci. Nanotechnol.* **2** 035009
[5] Bennett C H, Brassard G, Crepeau C, Jozsa R, Peres A and Wootters W K 1993 *Phys. Rev. Lett.* **70** 1895
[6] An N B 2009 *J. Phys. B: At. Mol. Opt. Phys.* **42** 125501
[7] Hou K, Wang J, Lu Y L and Shi S H 2009 *Int. J. Theor. Phys.* **48** 2005
[8] Luo M X, Chen X B, Ma S Y, Niu X X and Yang Y X 2010 *Opt. Commun.* **283** 4796
[9] Chen Q Q, Xia Y, Song J and An N B 2010 *Phys. Lett.* A **374** 4483
[10] An N B 2010 *Opt. Commun.* **283** 4113
[11] An N B, Bich C T and Don N V 2011 *Phys. Lett.* A **375** 3570
[12] An N B, Bich C T and Don N V 2011 *J. Phys. B: At. Mol. Opt. Phys.* **44** 135506
[13] Chen Q Q, Xia Y and An N B 2011 *Opt. Commun.* **284** 2617
[14] Wang Z Y 2011 *Int. J. Quantum Inf.* **9** 809
[15] Hou K, Li Y B, Liu G H and Sheng S Q 2011 *J. Phys. A: Math. Theor.* **44** 255304
[16] Xiao X O, Liu J M and Zeng G 2011 *J. Phys. B: At. Mol. Opt. Phys.* **44** 075501
[17] Bich C T, Don N V and An N B 2012 *Int. J. Theor. Phys.* **51** 2272
[18] Luo M X, Peng J Y and Mo Z W 2013 *Int. J. Theor. Phys.* **52** 644
[19] Zhan Y B and Ma P C 2013 *Quantum Inf. Process.* **12** 997
[20] Zhan Y B, Fu H, Li X W and Ma P C 2013 *Int. J. Theor. Phys.* **52** 2615
[21] Long L R, Zhou P, Li Z and Yin C L 2012 *Int. J. Theor. Phys.* **51** 2438
[22] Wang D and Ye L 2012 *Int. J. Theor. Phys.* **51** 3376
[23] Liao Y M, Zhou P, Qin X C and He Y H 2014 *Quantum Inf. Process.* **13** 615
[24] Cao T B, Nguyen V H and Nguyen B A 2016 *Adv. Nat. Sci.: Nanosci. Nanotechnol.* **7** 025007
[25] Luo M X, Chen X B, Yang Y X and Niu X X 2012 *Quantum Inf. Process.* **11** 751
[26] Yu R F, Lin Y J and Zhou P 2016 *Quantum Inf. Process.* **15** 4785
[27] Bennett C H, Brassard G, Popescu S, Schumacher B, Smoin J A and Wootters W K 1996 *Phys. Rev. Lett.* **76** 722
[28] Pan J W, Simon C, Brukner C and Zeilinger A 2001 *Nature* **410** 1067
[29] Romero J L, Roa L, Retamal J C and Saavedra C 2002 *Phys. Rev.* A **65** 052319
[30] Bouda J and Buzek V 2002 *Phys. Rev.* A **65** 034304
[31] Brun T A, Caves C M and Schack R 2001 *Phys. Rev.* A **63** 042309
[32] Liang H Q, Liu J M, Feng S S and Chen J G 2011 *J. Phys. B: At. Mol. Opt. Phys.* **44** 115506
[33] Chen Z F, Liu J M and Ma L 2014 *Chin. Phys.* B **23** 020312
[34] Li J F, Liu J M and Xu X Y 2015 *Quantum Inf. Process.* **14** 3465

Adv. Nat. Sci.: Nanosci. Nanotechnol. **8** (2017) 015012

V H Nguyen *et al*

[35] Liang H Q, Liu J M, Feng S S, Chen J G and Xu X Y 2015 *Quantum Inf. Process.* **14** 3857
[36] Fortes R and Rigolin G 2015 *Phys. Rev.* A **92** 012338
[37] Wang M M and Qu Z G 2016 *Quantum Inf. Process.* **15** 4805
[38] Greenberger D M, Horne M A and Zeilinger A 1989 Going beyond Bell's theorem *Bell's Theorem, Quantum Theory and Conception of the Universe* (Amsterdam: Springer) pp 69–72
[39] Kraus K 1983 *States, Effects and Operations: Fundamental Notions of Quantum Theory* (Berlin: Springer)
[40] Nielsen M A and Chuang I L 2000 *Quantum Computation and Quantum Information* (Cambridge: Cambridge University Press)
[41] Bruß D and Macchiavello C 1999 *Phys. Lett.* A **253** 249
[42] Badziag P, Horodecki M, Horodecki P and Horodecki R 2000 *Phys. Rev.* A **62** 012311